Cosmic Masers - from OH to H_0
Proceedings IAU Symposium No. 287, 2012
R.S. Booth, E.M.L. Humphreys & W.H.T. Vlemmings, eds.

doi:10.1017/S1743921312006618

Polarization of Class I methanol (CH_3OH) masers

A. P. Sarma
DePaul University, Chicago IL, USA
email: asarma@depaul.edu

Abstract. Magnetic fields are known to play an important role in several stages of the star formation process. Class I methanol (CH_3OH) masers offer the possibility of measuring the large-scale magnetic field in star forming regions at high angular resolution, due to connections between the large-scale magnetic field in the pre-shock regions to the observed magnetic field along the outflows in the post-shock regions where these masers are formed. The detection of the Zeeman effect in the 36 GHz and 44 GHz Class I methanol maser lines by Sarma and Momjian has opened an exciting new window into the study of the star formation process, but for the results to be interpreted correctly, the Zeeman splitting factor (z) for both these lines needs to be urgently measured by experiment. Ratios between the pre-shock and post-shock magnetic fields and densities lead to the conclusion that the value of z cannot be too different from 1 Hz mG^{-1}, unless the predicted densities at which 36 GHz and 44 GHz methanol masers are excited are drastically incorrect. Similarities between the detected fields in 36 GHz and 44 GHz Class I masers, and 6.7 GHz Class II masers, support the claim that these masers may be tracing the large-scale magnetic field or that the magnetic field remains the same during different evolutionary stages of the star formation process, provided such similarities are not just due to the assumption of a uniform nominal value for z, or result simply from selection effects due to orientation and/or the shock process. Given the exciting possibilities, a larger statistical sample of measurements in both the 36 GHz and 44 GHz lines is certainly needed.

Keywords. magnetic fields — masers — polarization — stars: formation — radio lines: ISM

1. Introduction

Magnetic fields in star forming regions present tremendous observational and theoretical challenges. Incorporating them into numerical models significantly increases the computational complexity. Observing them requires high sensitivity and, if they are to be of any use in understanding star formation processes, high angular resolution. Yet, they are believed to play such important roles in a number of stages in the star formation process that measuring them and understanding their influence is of paramount importance. As it stands, the role of magnetic fields in regulating the onset of star formation is still a matter of debate (e.g., Crutcher *et al.* 2009). It has become increasingly clear, though, that magnetic fields play a critical role in carrying angular momentum away from the protostar during collapse (McKee & Ostriker 2007, and references therein). Moreover, the outflows along which this takes place may be driven by dynamically enhanced magnetic fields in the protostellar disk (Banerjee & Pudritz 2006). In particular, the driving of outflows along magnetic field lines may be critical in allowing accretion to continue onto high mass protostars (Banerjee & Pudritz 2007).

The Zeeman effect remains the most direct method for measuring the magnetic field strength (Troland *et al.* 2008). Over the years, observations of the Zeeman effect in H I and OH thermal lines have revealed the strength of the magnetic field in the lower density envelopes of molecular clouds (e.g., Brogan & Troland 2001; Sarma *et al.* 2000). However,

measuring fields in the dense gas nearer to the protostar is difficult to achieve with such lines. Thermal lines of CN hold promise (Falgarone *et al.* 2008), but must await the advent of high sensitivity and high angular resolution interferometers at their frequencies. On the other hand, interstellar masers, being compact and intense, offer a means of measuring the magnetic field in star forming regions at high angular resolution. For years, their effectiveness as probes of star forming regions was overshadowed by a perception that the specialized conditions in which such masers form necessarily prevented them from being linked to conditions on larger scales. However, recent discoveries indicate that rather than being a measure in isolated atypical fragments, the magnetic fields measured in masers are indeed linked to the larger scale magnetic field. Fish & Reid (2006) found a relative consistency in the magnetic fields measured in clusters of mainline (1665 and 1667 MHz) OH masers across a massive star forming region, and concluded that magnetic fields are ordered in massive star forming regions. More recently, Vlemmings *et al.* (2010) have determined from polarization observations of 6.7 GHz methanol masers toward Cepheus HW2 that the masers probe the large scale magnetic field.

It is in this context that the ability to measure the Zeeman effect in Class I methanol (CH_3OH) masers provides an important new tool. Historically, Class I methanol masers were categorized on the basis of their distance from observable indicators of star formation, whereas Class II methanol masers were known to be close to many of the acknowledged indicators of star formation (Menten 1991). Further study led to the conclusion that Class I methanol masers likely form in collisional shocked regions in protostellar outflows (Cragg *et al.* 1992; Sandell *et al.* 2005). Therefore, they offer us the potential to measure the magnetic field along the outflow. Of course, the effort to measure magnetic fields using these masers is still in its infancy, and this cherished goal will require sustained effort. Sarma & Momjian (2009) made the first measurement of the Zeeman effect in the 36 GHz Class I methanol maser line toward the star forming region M8E. Sarma & Momjian (2011) made the first measurement of the Zeeman effect in the 44 GHz Class I methanol maser line toward a star forming region in OMC-2. This contribution will discuss these discoveries, and what they tell us about the potential for learning about star forming regions by making polarization observations of Class I methanol masers.

2. Observations and Data Reduction

Observations of the $4_{-1} - 3_0\, E$ methanol maser emission line at 36 GHz toward M8E were carried out in the C-configuration of the Expanded Very Large Array (EVLA) of the NRAO† in two 2 hr sessions on 2009 July 9 and 25. Thirteen EVLA antennas equipped with the 27−40 GHz (Ka-band) receivers were used in these observations. Meanwhile, observations of the $7_0 - 6_1\, A^+$ methanol maser emission line at 44 GHz were carried out using 22 antennas in the D-configuration of the EVLA in two 2 hr sessions on 2009 Oct 25 and Nov 25. Table 1 lists the observing parameters and other relevant data for these observations. Both the 36 GHz and 44 GHz data were correlated using the old VLA correlator, and in order to avoid the aliasing known to affect the lower 0.5 MHz of the bandwidth for EVLA data correlated with the old VLA correlator, the spectral line was centered in the second half of the 1.56 MHz wide band. For the 36 GHz observations toward M8E, the source 3C286 (J1331+3030) was used to set the absolute flux density scale, while the compact source J1733−1304 was used as an amplitude calibrator. For the 44 GHz observations toward OMC-2, the source 3C147 (J0542+4951) was used to

† The National Radio Astronomy Observatory (NRAO) is a facility of the National Science Foundation of the USA operated under cooperative agreement by Associated Universities, Inc.

https://doi.org/10.1017/S1743921312006618 Published online by Cambridge University Press

Table 1. Parameters for EVLA Observations

Parameter	**36 GHz Observations**	**44 GHz Observations**
Observation Dates	2009 July 9 & 25	2009 Oct 25 & Nov 25
Configuration	C	D
R.A. of field center (J2000)	$18^{\rm h}04^{\rm m}53.3^{\rm s}$	$05^{\rm h}35^{\rm m}27.66^{\rm s}$
Decl. of field center (J2000)	$-24°26'42.0''$	$-05°09'39.6''$
Total Bandwidth	1.56 MHz	1.56 MHz
No. of channels	256	256
Channel Spacing	0.051 km s^{-1}	0.040 km s^{-1}
Total Observing Time	2 hr	4 hr
Rest Frequency	36.16929 GHz	44.069488 GHz
Velocity at band center[a]	13.7 km s^{-1}	13.2 km s^{-1}
Target source velocity	11.2 km s^{-1}	11.6 km s^{-1}
FWHM of synthesized beam	$1.76'' \times 0.58''$	$1.93'' \times 1.58''$
	P.A. $= -7.80°$	P.A. $= -10.40°$
Line rms noise[b]	18 mJy beam^{-1}	8 mJy beam^{-1}

Notes: [a] The line was centered in the second half of the 1.56 MHz band in order to avoid aliasing (see § 2).
[b] The line rms noise was measured from the stokes I image cube using maser line free channels.

set the absolute flux density scale, while the compact source J0607−0834 was used as an amplitude calibrator.

The editing, calibration, Fourier transformation, deconvolution, and processing of the data were carried out using the Astronomical Image Processing System (AIPS) of the NRAO. After applying the amplitude gain corrections of J1733−1304 on the target source M8E, and J0607−0834 on the target source OMC-2 respectively, the spectral channel with the strongest maser emission signal in each of the two sets of data was split, then self-calibrated in both phase and amplitude in a succession of iterative cycles (e.g., Sarma *et al.* 2002). The final phase and amplitude solutions were then applied to the full spectral-line uv data set, and Stokes I and V image cubes were made with a synthesized beamwidth of $1.76'' \times 0.58''$ for M8E and $1.93'' \times 1.58''$ for OMC-2 respectively. Further processing of the data, including magnetic field estimates, was done using the MIRIAD software package.

3. Analysis

For cases in which the Zeeman splitting $\Delta\nu_z$ is much less than the line width $\Delta\nu$, the magnetic field can be obtained from the Stokes V spectrum, which exhibits a *scaled derivative* of the Stokes I spectrum (Heiles *et al.* 1993). Here, consistent with AIPS conventions, I = (RCP+LCP)/2, and V = (RCP−LCP)/2; RCP is right- and LCP is left-circular polarization incident on the antennas, where RCP has the standard radio definition of clockwise rotation of the electric vector when viewed along the direction of wave propagation. Since the observed V spectrum may also contain a scaled replica of the I spectrum itself, the Zeeman effect can be measured by fitting the Stokes V spectra in the least-squares sense to the equation

$$V = aI + \frac{b}{2}\frac{\mathrm{d}I}{\mathrm{d}\nu} \tag{3.1}$$

(Troland & Heiles 1982; Sault *et al.* 1990). The fit parameter a is usually the result of small calibration errors in RCP versus LCP, and is expected to be small. In both the 36 GHz and 44 GHz observations, a was of the order of 10^{-4} or less. While eq. (3.1) is strictly true only for thermal lines, numerical solutions of the equations of radiative

https://doi.org/10.1017/S1743921312006618 Published online by Cambridge University Press

transfer (e.g., Nedoluha & Watson 1992) have shown that it gives reasonable values for the magnetic fields in masers also. In eq. (3.1), the fit parameter $b = zB\cos\theta$, where z is the Zeeman splitting factor (Hz mG^{-1}), B is the magnetic field, and θ is the angle of the magnetic field to the line of sight (Crutcher *et al.* 1993). For all cases in which $\Delta\nu_z \ll \Delta\nu$, the Zeeman effect reveals information only on the magnetic field along the line of sight, $B_{\rm los} = B\cos\theta$.

The value of the Zeeman splitting factor z is critical for determining $B_{\rm los}$ from the observations. Clearly, z for methanol masers is very small, because CH_3OH is a non-paramagnetic molecule. Unfortunately, there are no existing laboratory measurements for z at either 36 GHz or 44 GHz. Following the treatment of Vlemmings (2008) for the Zeeman splitting of 6.7 GHz methanol masers, Sarma & Momjian (2009) derived z for the 36 GHz CH_3OH line using the Landé g-factor based on laboratory measurements of 25 GHz methanol masers (Jen 1951). However, Vlemmings *et al.* (2011) has since reported that such an extrapolation is likely to give a value of z that is in error by a factor of 2-10, depending on the methanol ladder (E or A). Therefore, it is best to refrain from quoting a value for $B_{\rm los}$ in this contribution, pending experimental measurement of the z factor. Instead, the values for $zB_{\rm los}$ will be stated, since they come directly from the observed data, and are not affected by any estimated value of z.

4. Results and Discussion

4.1. *Zeeman detection toward M8E at 36 GHz*

Figure 1 shows the Stokes I and V profiles in the 36 GHz Class I methanol maser line toward two positions in M8E; the two positions are to the northwest and southeast of the maser line peak. As described in § 3, the magnetic fields were determined by fitting the Stokes V spectra in the least-squares sense using equation (3.1). The values of the parameter b in eq. (3.1) obtained from this fit are $b = -53.2 \pm 6.0$ Hz for the northwest position, and $b = +34.4 \pm 5.9$ Hz for the southeast position. Since an experimentally measured value of z is not available, it is difficult to convert this result into a value for the magnetic field. Still, we can speculate that the true (experimentally determined) value of z for the 36 GHz line will not be too different from $\sim$1 Hz mG^{-1}, based on the discussion in § 4.3 below.

The line-of-sight magnetic field in M8E has opposite signs at the two positions for which Stokes I and V profiles are shown in Fig. 1; this is true irrespective of the eventually determined value of z. By convention, a negative value for $B_{\rm los}$ indicates a field pointing toward the observer. The observed change in the sign of $B_{\rm los}$ at these two positions, together with a slight asymmetry in the maser line profiles at each position, indicates that we are observing at least two masers that are very close in position and velocity. The masers are marginally resolved in these C-configuration observations, otherwise the opposite magnetic fields would sum to zero. EVLA B- or A-configuration observations will be necessary to fully resolve the maser components; Sarma & Momjian have an approved proposal for follow-up observations. The observed change in the sign of $B_{\rm los}$ occurs over a size scale of $0.9''$, equal to 1300 AU (assuming the distance to M8E is 1.5 kpc). This may mean that the clumps where the 36 GHz maser is being excited come from two different regions where the field is truly different. Alternatively, it may mean that the field lines curve across the region in which the masers are being excited, so that the line-of-sight field traced by one maser is pointed toward us, whereas that traced by the other maser is pointed away from us.

https://doi.org/10.1017/S1743921312006618 Published online by Cambridge University Press

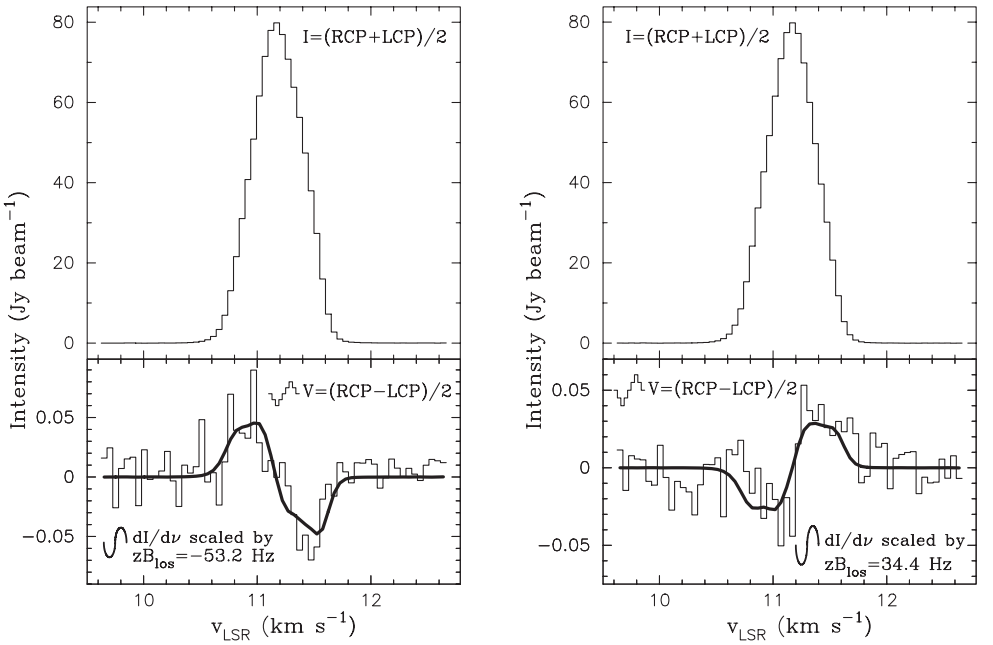

Figure 1. Stokes I (*top-histogram*) and V (*bottom-histogram*) profiles of the 36 GHz Class I methanol maser toward the northwest (*left panel*) and southeast (*right panel*) of the maser line peak in M8E. The curve superposed on V in each of the lower frames is the derivative of I scaled by a value of $zB_{\rm los} = -53.2 \pm 6.0$ Hz in the left panel, and $zB_{\rm los} = +34.4 \pm 5.9$ Hz in the right panel.

4.2. *Zeeman detection toward OMC-2 at 44 GHz*

Figure 2 shows the Stokes I and V profiles in the 44 GHz Class I methanol maser line toward OMC-2. Again, as described in § 3, the magnetic fields were determined by fitting the Stokes V spectra in the least-squares sense using equation (3.1). The value of the parameter b in eq. (3.1) obtained from this fit is equal to $b = 18.4 \pm 1.1$ Hz. As in the case for the 36 GHz line, it is difficult to derive a value for $B_{\rm los}$ without knowing the experimentally determined value for z. Once again, though, we can speculate that the true (experimentally determined) value of z for the 44 GHz line will not be too different from $\sim$1 Hz mG^{-1}, based on the discussion in § 4.3 below.

4.3. *Magnetic Fields and Densities*

Class I methanol masers are known to be excited in collisional shocks along outflows in star forming regions. This appears to be the case in OMC-2, where Slysh & Kalenskii (2009) observed six 44 GHz methanol masers spread out along a line aligned at an angle approximately 30° east of north, and at larger scales there is a CO outflow aligned along the same direction (Takahashi *et al.* 2008). Cyganowski *et al.* (this conference) have also shown several excellent examples of Class I methanol masers lined up along outflows at comparable (and high) resolution. Since maser amplification is particularly efficient in directions approximately perpendicular to the shock propagation, the compression of an ordered magnetic field from this orientation would give the following relationship:

$$\frac{B_0}{\rho_0} = \frac{B_1}{\rho_1} \tag{4.1}$$

https://doi.org/10.1017/S1743921312006618 Published online by Cambridge University Press

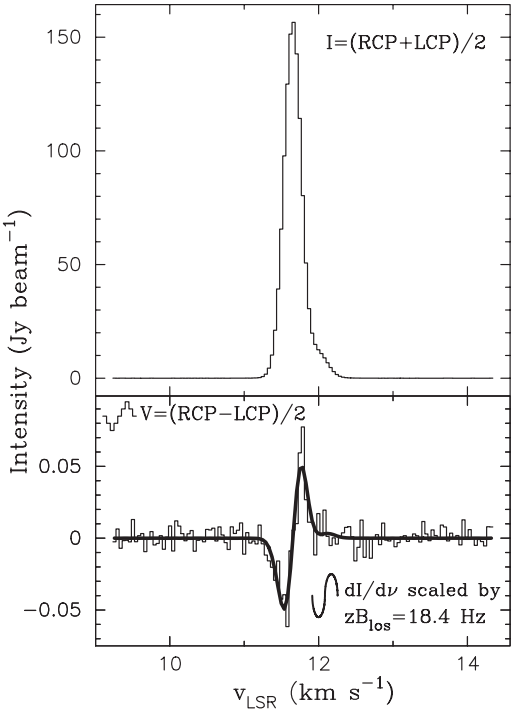

Figure 2. Stokes I (*top-histogram*) and V (*bottom-histogram*) profiles of the 44 GHz Class I methanol maser in OMC-2. The curve superposed on V in the lower frame is the derivative of I scaled by a value of $zB_{\rm los} = 18.4 \pm 1.1$ Hz.

where 0 and 1 refer to the preshock and postshock (maser) regions respectively, and ρ is the gas density (e.g., Sarma *et al.* 2008). The discussion below uses the molecular hydrogen number density n instead of ρ. If B_0 and n_0 are known, then the measured value of $B_{\rm los}$ can be used to find n_1, and compared to the density at which the 44 GHz methanol maser is known to be excited. Poidevin *et al.* (2010) used the Chandrasekhar-Fermi method to estimate the value of the magnetic field in this region from their 850 μm observations, and found it to be 0.13 mG; this is adopted as the value of B_0 in equation (4.1). The value $n_0 = 10^4$ cm^{-3} can be taken from the C^{18}O observations toward OMC-2 by Castets & Langer (1995). Finally, $B_1 = 2\,B_{\rm los}$ can be written based on statistical grounds (Crutcher 1999). While the current observations only give the value of $zB_{\rm los}$, and $B_{\rm los}$ cannot be obtained from observations without knowing z (§ 3), a nominal value of $z = 1.0$ Hz mG^{-1} provides some interesting insights. Using these values in equation (4.1), one obtains $n_1 \sim 10^6$ cm^{-3} for the postshock number density. This is in excellent agreement with theoretical models that show the 44 GHz methanol maser action is maximized in regions with density $10^5 - 10^6$ cm^{-3} (Pratap *et al.* 2008, and references therein). This implies that when the value of z is eventually measured experimentally, it will likely not turn out to be too different from 1.0 Hz mG^{-1}, unless there is something drastically wrong with the theoretically predicted densities at which the 44 GHz maser is excited. Similar considerations apply to the value of z for the 36 GHz line.

4.4. *Additional Considerations and Future Directions*

While two examples, each at a different frequency, are far from the final word on a subject, there is no denying that the prospect of measuring the Zeeman effect in Class

https://doi.org/10.1017/S1743921312006618 Published online by Cambridge University Press

I methanol masers opens up an exciting new window into the physics of star formation. Turning equation (4.1) around, one could say that knowing n_0 from observations and n_1 from theoretical models for methanol masers, the measured values of $B_{\rm los}$, and hence B_1, would allow us to get a measure of the large-scale magnetic field B_0. This opens up the possibility of tracking the large scale magnetic field in star forming regions at high angular resolution by observing the Zeeman effect in Class I methanol masers. Moreover, the $B_{\rm los}$ values observed in the 36 GHz and 44 GHz lines (based on a nominal value of $z \sim 1$ Hz mG^{-1}) appear to be very similar to the $B_{\rm los}$ values observed in the 6.7 GHz Class II methanol maser line observed by Vlemmings (2008) and Vlemmings *et al.* (2011), who detected significant magnetic fields with the 100 m Effelsberg telescope in this line toward 44 sources. Since Class I and Class II methanol masers likely trace different spatial regions (Ellingsen 2005, and references therein), the likely similarities in the fields measured in these masers provide additional support for the claim that methanol masers may trace the larger scale magnetic fields in star forming regions. Another possibility might be that Class I masers occur in the very early stages of star formation (before the formation of an ultracompact H II region), and Class II masers occur later on in the evolutionary process. In that case, the similarity in $B_{\rm los}$ for these two classes may indicate that the magnetic field strength remains the same during the early stages of the star formation process. It is possible, however, that the similarities are simply due to the nominal choice of $z \sim 1$ Hz mG^{-1} for the 36 GHz and 44 GHz lines or, even if the value of z may really be similar for these two lines (which appears likely based on the discussion in § 4.3), that the similarities in measured magnetic fields may result simply from selection effects due to orientation and/or the shock process. Moving forward, of course, it is important to dwell on alternative possibilities, if for nothing else than to maintain a healthy dose of scientific skepticism until overwhelming examples point to the contrary. Ascribing the detections to a completely fake Zeeman pattern does not appear to be a possibility, especially given that the detections have been made at different frequencies (hence different receivers), and the Class II detections are even by another class of telescope. Moreover, detections taken on different days were imaged separately in order to verify that similar Stokes V patterns were obtained from different sets of observations. Next, if the experimentally measured value of z turns out to be a factor of 10 lower than the nominal value of 1 Hz mG^{-1}, the calculated magnetic fields would be too large, and some kind of non-Zeeman interpretation would have to be ascribed to the detected Stokes V profile. Such considerations certainly make the case for a larger statistical sample of measurements in both the 36 GHz and 44 GHz lines. Perhaps even more critical are experimental measurements of the Zeeman splitting factor z for both the 36 GHz and 44 GHz lines (and 6.7 GHz lines), in order to test possible correlations or anti-correlations between fields measured in Class I and II masers and at different frequencies within each of these types.

5. Conclusions

The detection of the Zeeman effect in the 36 GHz and 44 GHz Class I methanol (CH_3OH) maser lines opens a new window into the star formation process. Given the connections between pre-shock and post-shock magnetic fields and the densities in these regions, the magnetic fields detected in these lines could potentially be used to trace the large-scale magnetic field at high spatial resolution in star forming regions. At present, the Zeeman splitting factor z for both these lines has not been measured experimentally, and this complicates the interpretation of the 36 GHz and 44 GHz detections. The assumption of a nominal value of $z = 1$ Hz mG^{-1} for the 36 GHz and 44 GHz lines reveals that the

https://doi.org/10.1017/S1743921312006618 Published online by Cambridge University Press

magnetic fields near the protostar (as traced by Class II masers) may be similar to fields farther away along the outflow (as traced by Class I methanol masers), provided this similarity is not merely due to the adoption of a uniform nominal value for z, or at at deeper level, due to selection effects resulting from orientation and/or the shock process itself. However, if z is significantly different from this value, considerations of the ratio of magnetic fields to densities in pre-shock and post-shock regions indicates that models for the densities at which 36 GHz and 44 GHz methanol masers are excited would have to be significantly revised. All of this points to the urgent need for the experimental measurement of z and motivates a larger statistical sample of measurements in both the 36 GHz and 44 GHz Class I methanol maser lines.

References

Banerjee, R. & Pudritz, R. E. 2006, *ApJ*, 641, 949
Banerjee, R. & Pudritz, R. E. 2007, *ApJ*, 660, 479
Brogan, C. L. & Troland, T. H. 2001, *ApJ*, 560, 821
Castets, A. & Langer, W. D. 1995, *A&A*, 294, 835
Cragg, D. M., Johns, K. P., Godfrey, P. D., & Brown, R. D. 1992, *MNRAS*, 259, 203
Crutcher, R. M., Troland, T. H., Goodman, A. A., Heiles, C., Kazes, I., & Myers, P. C. 1993, *ApJ*, 407, 175
Crutcher, R. M. 1999, *ApJ*, 520, 706
Crutcher, R. M., Hakobian, N., & Troland, T. H. 2009, *ApJ*, 692, 844
Ellingsen, S. P. 2005, *MNRAS*, 359, 1498
Falgarone, E., Troland, T. H., Crutcher, R. M., & Paubert, G. 2008, *A&A*, 487, 247
Fish, V. L. & Reid, M. J. 2006, *ApJS*, 164, 99
Heiles, C., Goodman, A. A., McKee, C. F., & Zweibel, E. G. 1993, in *Protostars and Planets III*, ed. E. H. Levy & J. I. Lunine (Tucson: Univ. Arizona Press), 279
Jen, C. K. 1951, *Physical Review*, 81, 197
McKee, C. F. & Ostriker, E. C. 2007, *ARAA*, 45, 565
Menten, K. M. 1991, *ApJL*, 380, L75
Nedoluha, G. E. & Watson, W. D. 1992, *ApJ*, 384, 185
Poidevin, F., Bastien, P., & Matthews, B. C. 2010, *ApJ*, 716, 893
Pratap, P., Shute, P. A., Keane, T. C., Battersby, C., & Sterling, S. 2008, *AJ*, 135, 1718
Sandell, G., Goss, W. M., & Wright, M. 2005, *ApJ*, 621, 839
Sarma, A. P., Troland, T. H., Roberts, D. A., & Crutcher, R. M. 2000, *ApJ*, 533, 271
Sarma, A. P., Troland, T. H., Crutcher, R. M., & Roberts, D. A. 2002, *ApJ*, 580, 928
Sarma, A. P., Troland, T. H., Romney, J. D., & Huynh, T. H. 2008, *ApJ*, 674, 295
Sarma, A. P. & Momjian, E. 2009, *ApJL*, 705, L176
Sarma, A. P. & Momjian, E. 2011, *ApJL*, 730, L5
Sault, R. J., Killeen, N. E. B., Zmuidzinas, J., & Loushin, R. 1990, *ApJS*, 74, 437
Slysh, V. I. & Kalenskii, S. V. 2009, *Astronomy Reports*, 53, 519
Takahashi, S., Saito, M., Ohashi, N., Kusakabe, N., Takakuwa, S., Shimajiri, Y., Tamura, M., & Kawabe, R. 2008, *ApJ*, 688, 344
Troland, T. H. & Heiles, C. 1982, *ApJ*, 252, 179
Troland, T. H., Heiles, C., Sarma, A. P., Ferland, G. J., Crutcher, R. M., & Brogan, C. L. 2008, arXiv:0804.3396
Vlemmings, W. H. T. 2008, *A&A*, 484, 773
Vlemmings, W. H. T., Surcis, G., Torstensson, K. J. E., & van Langevelde, H. J. 2010, *MNRAS*, 404, 134
Vlemmings, W. H. T., Torres, R. M., & Dodson, R. 2011, *A&A*, 529, A95

https://doi.org/10.1017/S1743921312006618 Published online by Cambridge University Press